## COMPUTATIONAL FLUID DYNAMICS CALIBRATION OF TATTERSALL MK-II TYPE RHEOMETER FOR CONCRETE

H.D. Le<sup>1,2\*</sup>, G. De Schutter<sup>1</sup>, E.H. Kadri<sup>2</sup>, S. Aggoun<sup>2</sup>, J. Vierendeels<sup>4</sup>, S. Tichko<sup>1,3</sup>, AND P. TROCH3

<sup>1</sup>Magnel Laboratory for Concrete Research, Department of Structural Engineering, Ghent University, 9000 Ghent, Belgium

<sup>2</sup> Laboratory for Mechanics and Materials in Civil Engineering, Department of Civil Engineering, Unit of Formation and Research Science and Technology, Cergy-Pontoise University, 95000 Pontoise, France

<sup>3</sup> Hydraulics Laboratory, Department of Civil Engineering, Ghent University,9000 Ghent, Belgium

<sup>4</sup> Department of Flow, Heat and Combustion Mechanics, Ghent University, 9000 Ghent, Belgium

\*Corresponding author: haidang.le@ugent.be Fax: x32.9.245845

Received: 1.10.2012, Final version: 21.2.2013

Currently more and more researches have been performing concerning the numerical simulation of the behavior of fresh concrete during pumping or formwork filling. Adequate implementation of the rheology properties of fresh concrete is a determinant key to obtain realistic simulations. However, in many cases, the rheological parameters of the fresh concrete as determined by rheometers are not sufficiently accurate. The common principle of all the rheometers is not to measure directly the rheological parameters of concrete but to measure some basic physical parameters (torque, velocity, pressure, ...) that that in some cases allow the calculation of the rheological parameter in terms of fundamental physical quantities. Errors can be caused by undesired flow phenomena which are not taken into the prediction formulas and by the inaccurate prediction formulas themselves. This is directly related to the poor calibration of the rheometer that cannot cover all ranges of materials. This paper investigates the calibration of the Tattersall MK-II rheometer by performing the numerical simulation for a tremendous range of concrete flowing in the rheometer, using computational fluid dynamics (CFD). This allows to quickly and accurately obtain the rheological properties of fresh concrete, which can then be used consistently for further flow simulations. This method can be applied for all types of rheometer.

#### **ZUSAMMENFASSUNG:**

Gegenwärtig werden immer mehr Arbeiten über die numerische Simulation des Verhaltens frischen Betons während des Pump- oder Füllvorganges bei der Schalung durchgeführt. Eine adäquate Implementation der rheologischen Eigenschaften des frischen Betons ist essentiell, um realistische Simulationen durchzuführen. Jedoch sind die rheologischen Größen des frischen Betons, die mittels rheometrischer Messungen erhalten wurden, in vielen Fällen nicht ausreichend genau. Das gemeinsame Prinzip aller Rheometer besteht darin, nicht direkt die rheologischen Parameter des Betons zu messen. Statt dessen werden einige grundlegende physikalische Größen (Drehmoment, Geschwindigkeit, Druck, ...) ermittelt, die in einigen Fällen erlauben, die rheologischen Parameter mit Hilfe fundamentaler physikalischer Größen zu berechnen. Fehler können dabei durch nicht gewünschte Strömungsphänomene verursacht werden, die in den Formeln nicht berücksichtigt werden. Dies wird direkt in den Zusammenhang mit der mangelhaften Kalibrierung von Rheometern gebracht, die nicht den gesamten Materialbereich erfassen kann. In dieser Arbeit wird die Kalibrierung eines Tattersall MK-II-Rheometers untersucht. Dabei werden numerische Computational Fluid Dynamics (CFD)-Simulationen über einen sehr großen Bereich einer Betonströmung in dem Rheometer durchgeführt. Dies erlaubt, schnell und genau die rheologischen Eigenschaften vom frischen Beton zu gewinnen, die für weitere Strömungssimulationen verwendet werden können. Diese Methode kann auf alle Rheometer angewandt werden.

#### RÉSUMÉ:

De nos jours, des simulations numériques du comportement du ciment frais durant le pompage et le remplissage de pré-formes sont de plus en plus entreprises. L'implémentation correcte des propriétés rhéologiques du ciment frais est la clé déterminante afin d'obtenir des simulations réalistes. Cependant, dans beaucoup de cas, les paramètres rhéologiques obtenus à l'aide de rhéomètres ne sont pas suffisamment précis. Le principe commun de tous les rhéomètres n'est pas de mesurer directement les paramètres rhéologiques du ciment, mais de mesurer des paramètres physiques basiques (torsion, vitesse, paramètres rhéologiques sous forme de quantités physiques fondamentales. Les sources d'erreurs peuvent provenir de phénomènes d'écoulement non désirés qui ne sont pas

© Appl. Rheol. 23 (2013) 34741 DOI: 10.3933/ApplRheol-23-34741 tenus en compte par les formules de prédiction, ou de l'imprécision des formules elles mêmes. Ceci est directement associé à la calibration médiocre du rhéomètre qui ne peut pas couvrir tous les types de matériaux. Cet article étudie la calibration du rhéomètre Tattersall MK-II en effectuant la simulation numérique d'une très grande variété de ciments en écoulement dans le rhéomètre, en utilisant un programme de dynamique des fluides. Ceci permet d'obtenir rapidement et de manière précise les propriétés rhéologiques du ciment frais, qui peuvent ensuite être utilisées de manière consistante pour des simulations supplémentaires d'écoulement. Cette méthode peut être appliquée à tous types de rhéomètres.

KEY WORDS: rheometer, CFD, calibration, shear flow, Bingham, Herschel-Bulkley, Fluent

#### 1 INTRODUCTION

For the objective of measuring the rheological properties of concrete, many rheometers have been developed around the world [1-5]. In order to deal with different disturbing phenomena such as bottom effect, secondary flow, plug flow, gravity segregation [6], wall slip, ..., many mechanical solutions have been worked out. The general principle of these rheometers converges to determining the relationship between a parameter related to shear stress (mostly torque) and a parameter related to shear rate (mostly rotational speed) which is the T- $\Omega$  curve where T is the torque and  $\Omega$  is the rotational speed. After this basic step, the method used to "translate" this relationship to shear stress-shear rate relationship  $(\tau - \dot{\gamma})$  curve (where  $\tau$  is the shear stress and  $\dot{\gamma}$  is the shear rate) starts to diverge a lot from one rheometer to another depending on their mechanical solution [1, 2, 7-11]. The Tattersall MK-II rheometer has a good mechanical solution to deal with the gravity segregation which can in many cases be one of the most serious influence factors of the rheometry [12-14]. However, this mechanical solution based on the complex geometry of the vane implies that it is impossible to have an analytical solution for the T- $\Omega$ curve to  $\tau$  -  $\dot{\gamma}$  curve translation [10]. Therefore, a computational fluid dynamics calibration method combined with mathematical regression modeling has been developed to determine the translation in question. The method takes into account the errors resulting from bottom effect, secondary flow and plug flow.

# 2 RHEOLOGICAL BEHAVIOR OF CONCRETE

It has been reported in the literature that the rheological properties of fresh concrete can be described using at least two parameters: Yield stress  $\tau_o$  and plastic viscosity [12, 15–18]. Those parameters are usually obtained from the linear relationship between shear stress  $\tau$  and shear rate  $\dot{\gamma}$  which is modeled by the Bingham fluid law. [10] Bingham model:

$$\tau = \tau_o + \mu \dot{\gamma} \tag{1}$$

However, recent research has shown nonlinear rheological behavior of fresh concrete, particularly shear thickening of self-compacting concrete [19] and shear thinning of cement paste [20]. Therefore, more general models that are able to describe both linear and nonlinear behavior were investigated like modified Bingham, biexponential or Herschel-Bulkley [16]. Although the Herschel-Bulkley model has some disadvantages including underestimation of the yield stress for shear thinning and overestimation in case of shear thickening, it remains the most frequently applied model in non-linear concrete rheology. Because of the availability of experimental data in literature [4], the Herschel-Bulkley relation will be applied in this paper. The Herschel-Bulkley model is expressed as:

$$\tau = \tau_o + k\dot{\gamma}^n \tag{2}$$

Where  $\tau$  denotes the shear stress,  $\tau_o$  the yield stress,  $\dot{\gamma}$  the shear rate, k the consistency index and n the power index. For Bingham material, n=1 and  $k=\mu$  is the plastic viscosity. For shear thickening material, n>1 and for shear thinning material n<1.

#### **3 CONCRETE RHEOMETRY**

Cement-paste, mortar and concrete contain solid particles in different size of aggregates. As a result, the free space to make the material flow

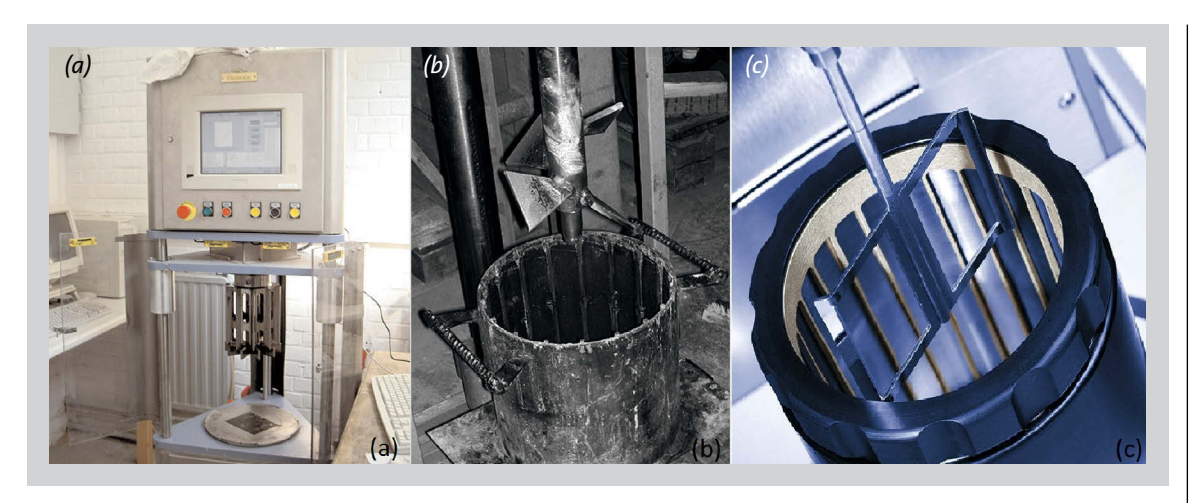


Figure 1:
(a) Contec viscometer,
(b) Tattersall rheometer,
and (c) Anton Paar MCR-52
rheometer.

must be sufficiently large. This also holds for the gap between shearing objects in a rheometer. On the other hand, the way the fluid flows in a rheometer must be studied in order to minimize segregation, plug flow, bottom effect, slip layer and secondary flow. As the requirement to have a sufficiently large gap is increasing the risk on having disturbing effects, it is difficult to design a rheometer that can be polyvalent for cement paste, mortar and different types of concrete. In this paper, for different study phases and different objectives, three rheometers have been considered: the Contec viscometer 5 (Figure 1a), the Tattersall MK-II (Figure 1b) and the Anton Paar MCR-52 (Figure 1c). These rheometers are based on the principle of concentric cylinders.

The geometry of the ConTec - BML viscometers (which will be named as ConTec viscometers from this point on) is based on the principle of concentric cylinders. The concrete is placed in a reservoir, of which its outer boundary forms the outer cylinder. The inner cylinder consists of two parts. The upper part is the part which measures the torque; the lower part does not participate in the measurements, in order to eliminate the influence of the complex 3-D flow pattern at the bottom of the rheometer. Both cylinders are equipped with vertical ribs in order to prevent wall slip. Several inner and outer cylinders with different heights and diameters are available. The rheometer used in this research project, being the ConTec Viscometer 5, has an outer cylinder with a radius of 14.5 cm, an inner cylinder with  $R_i = 10$  cm. The height of the inner cylinder submerged in the concrete measures 12.5 cm. The total volume of concrete needed in this rheometer is around 12-15 liter. In concrete rheometry field, the Contec viscometer family has actually become one of the most reliable rheometers because of its capabilities to minimize the bottom effect and the secondary flow and because of its simple geometry. Therefore, the analytical calculations of shear stress and shear rate from torque and rotational speed based on the geometry of the rheometer became

highly trustworthy. However, the effect of gravity-induced segregation cannot be taken into account by the analytical calculations and the effect of plug can be included, however time consuming.

The problems that the Contec viscometers are facing can be minimized by changing the way the material flows. In the Tattersall MK-II rheometer, the outer cylinder is formed by the concrete reservoir and it is equipped with ribs in order to prevent wall slip. The outer cylinder of the rheometer applied in this study measures 12.5 cm. In order to avoid gravity-induced segregation, the inner cylinder is equipped with an interrupted helical screw which mixes the concrete but it also gives the possibility to fall back between the blades. The distance between the outer edges (of the blades) of the inner cylinder measures 16 cm in horizontal direction and 14 cm in vertical direction. Nevertheless, because of the complex position of the blades, the disadvantages of this rheometer are well pronounced. Firstly, there is no algebraic calculation possible to calculate shear stress and shear rate from torque and rotational speed. As a consequence, a physical calibration was investigated by Feys et al. [10] allowing to calculate shear stress from torque and shear rate from rotational speed respectively. However, due to secondary flow of concrete through the blades, some data pretreatment has to be applied before calculating shear stress and shear rate. This data pretreatment process is only based on observations and measurements on oil and honey, without solid and fundamental physical meaning.

The mortar rheometer Anton Paar MCR-52 is equipped with an inner cylinder composed of four rectangular blades positioned in a cross-like form. The inner cylinder is 3 cm in diameter and 4.1 cm in height. The outer cylinder is equipped with ribs and is 7.4 cm in diameter. This rheometer has the advantage of very accurate measurement of torque and rotational speed and is used for a high range of fluids including mortar and cement paste. The disadvantages of this rheome-

ter are the wide gap that facilitates plug flow effect and bottom effect adding an extra torque to the torque calculated by the analytical solution. Four analytical approaches allow calculating the shear stress and shear rate from the torque and the rotational speed, as detailed hereafter. The first approach is based on the coaxial cylinders principles [20]. The requirement is that the velocity distribution must be linear, which can be fulfilled in case of a narrow gap. This requirement is not fully achieved in this case, resulting in a small error. The shear stress and shear rate are predicted using the following expressions:

$$\tau = \frac{R_i^2 + R_o^2}{4\pi h R_i^2 R_o^2} T \tag{3}$$

$$\dot{\gamma} = \frac{R_i^2 + R_o^2}{R_o^2 - R_i^2} \Omega \tag{4}$$

The second approach is also based on the same principles as the first approach, however with very low narrow gap  $(R_i/R_o > 0.99)$  [21]:

$$\tau = \frac{1}{2\pi h R_i^2} T$$

$$\dot{\gamma} = \frac{2}{\sqrt{1 - \frac{1}{2}}} \Omega$$
(5)

 $\dot{\gamma} = \frac{2}{R_i^2 \left( \frac{1}{R^2} - \frac{1}{R^2} \right)} \Omega$ (6)

The third approach is based on the Reiner-Riwlin equations which can be applied while assuming Bingham fluid behavior [22]:

$$\tau_o = \frac{G}{4\pi h} \left( \frac{1}{R_i^2} - \frac{1}{R_o^2} \right) \frac{1}{\ln \left( \frac{R_o}{R_i} \right)}$$
(7)

$$\mu = \frac{H}{8\pi^2 h} \left( \frac{1}{R_i^2} - \frac{1}{R_o^2} \right) \tag{8}$$

with  $\tau$  the shear stress (Pa),  $\dot{\gamma}$  the shear rate,  $\tau_{o}$ the yield stress (Pa),  $\mu$  the plastic viscosity (Pas), T the torque (Nm), C the rotational speed (rad/s), G the yield torque (Nm), H the slope of the  $T - \Omega$ curve (Nms),  $R_i$  the vane radius (m),  $R_o$  the outer cylinder radius (m), and h the vane height (m).

The fourth approach is based on the already mentioned Reiner-Riwlin equations combined with plug flow effect correction by an analytical iterative method.

#### **NUMERICAL SIMULATION**

#### 4.1 SIMULATION TOOL

The commercial ANSYS Fluent 12 computational fluid dynamics software is used for the simulations. By default, Fluent solves the equation of flows in a stationary reference frame. However, for the complex geometry moving part where the flow of fluid around the moving part is of interest, it is more advantageous to employ the sliding mesh technique. The technique consists of breaking the domain into multiple cell zones with defined interface between the cell zones then assigning the movement to the zone containing the moving part. In case of unsteady interaction between the stationary and moving parts, the Sliding Mesh approach is powerful to capture the transient behavior of the flow.

### 4.2 GOVERNING EQUATIONS FOR THE RHEO-**LOGICAL BEHAVIOR:**

For the non-Newtonian fluid, the shear stress can be written in terms of a non-Newtonian viscosi-

$$\overline{\overline{\tau}} = \eta(\overline{\overline{D}})\overline{\overline{D}}$$
 (9)

With  $\bar{\tau}$  is the extra stress tensor [23],  $\bar{D}$  the strain rate tensor [24]. However, in the non-Newtonian models available in FLUENT,  $\tau$  is considered to be a function of the shear rate  $\dot{\gamma}$  only, which is related to the second invariant of  $\bar{D}$  and is defined as

$$\dot{\gamma} = \sqrt{\frac{1}{2} \overline{\overline{D}} : \overline{\overline{D}}} \tag{10}$$

Therefore:

$$au = \eta(\dot{\gamma})\dot{\gamma}$$
 (11)

In this paper, we study concrete which is a non-Newtonian and possibly shear thickening fluid. The rheology of such materials is described by the Herschel Bulkley model. Theoretically, the value of the yield stress  $\tau_o$  plays the role of a discontinuous limit where for  $\tau < \tau_o$ , the material remains rigid,  $\dot{\gamma}=$  o and for  $\tau > \tau_o$ , the material flows as a power-law fluid,  $\dot{\gamma}$  > o. Due to this discontinuity at  $\dot{\gamma} = 0$ , it is impossible to implement the model into the Fluent solver without mathematical approximation. Therefore, a modification on the original Herschel-Bulkley law was implemented inside the fluent solver. The modified Herschel-Bulkley model considers an extra rheological parameter, the critical shear rate  $\dot{\gamma}_c$ (which does not have any physical meaning) in

$$\eta(\dot{\gamma}) = \frac{\tau_o}{\dot{\gamma}} \left( 2 - \frac{\dot{\gamma}}{\dot{\gamma}_c} \right) + k \left( (2 - n) + (n - 1) \frac{\dot{\gamma}}{\dot{\gamma}_c} \right)$$
(12)

the model of the viscosity  $\eta(\dot{\gamma})$  [25]. For  $\dot{\gamma} < \dot{\gamma}_c$ 

In combination with (Equation 11), this relation is resulting in:

$$\tau = \tau_o \left( 2 - \frac{\dot{\gamma}}{\dot{\gamma}_c} \right) + k \left( (2 - n) + (n - 1) \frac{\dot{\gamma}}{\dot{\gamma}_c} \right) \dot{\gamma}$$
(13)

For  $\dot{\gamma} > \dot{\gamma}_c$ 

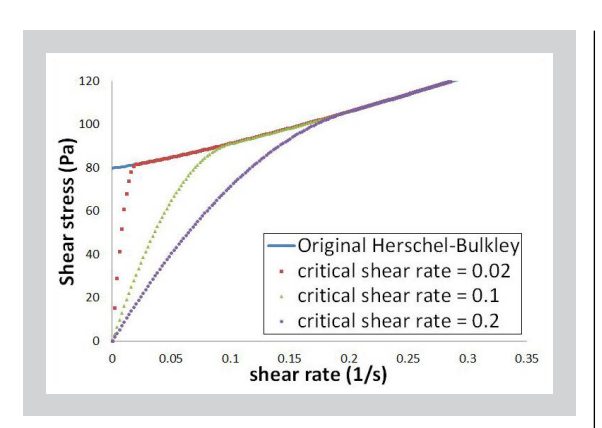
$$\eta(\dot{\gamma}) = \frac{\tau_o}{\dot{\gamma}} + k \left(\frac{\dot{\gamma}}{\dot{\gamma}_c}\right)^{n-1} \tag{14}$$

In combination with (Equation 11):

$$\tau = \tau_o + \frac{k}{\dot{\gamma}_c^{n-1}} \dot{\gamma}^n \tag{15}$$

As a result, the consistency index k in the original Herschel-Bulkley model is equivalent to the ratio  $k/\dot{\gamma}_{c}^{(n-1)}$  in the modified Herschel-Bulkley model. For example, for a Herschel-Bulkley material of  $\tau_o$  = 80 Pa, k = 180, n = 1.2, the value of consistency k given into Fluent must be  $180/\dot{\gamma}_{c}^{(n-1)}$ Pa depending on the personalized value of the critical shear rate.

According to this model, an ideal yield stress does not exist but there is a high consistency K second order shear thinning in the interval [o; critical shear rate value]. A lower critical shear rate leads to a better approximation of the original Herschel-Bulkley relation (Figure 2), but on



the other hand increases the calculation time to reach convergence. For all simulations in this paper, the critical shear rate is 0.001 1/s for all materials considered (yield stress varying from o to 800 Pa). This value is small enough to obtain reliable results, very close to the original Herschel-Bulkley behavior.

#### 4.3 SIMULATION PLAN

Within the simulations, two rheometers have been considered, namely The Contec viscometers 5 and the Tattersall MK-II. The simulation of the Contec viscometer 5 was studied because of the availability of experimental data which allow us to evaluate the difference between experiments and numerical simulation, in order to validate the numerical method. Once validated, the numerical method will be applied to the Tattersall MK-II rheometer.

As mentioned in the introduction, it is not possible to obtain an analytical solution for the conversion of the measured data (torque and rotational speed) to fundamental physical quantities (yield stress  $\tau_o$  and plastic viscosity  $\mu$  in case of the Bingham material or yield stress  $\tau_o$ , consistency k, and flow index n in case of the Herschel Bulkley material). However, the problem can be circumvented by an alternative method which consists of doing numerical tests – a method developed by Wallevik J.E. on his research for the COPLATE rheometer [26]. The so-called numerical tests consist of doing series of simulations in which the rheological parameters of the fluid  $(\tau_o, k, \text{ and } n)$  are varied. For each variation, the corresponding torque-rotational speed relationship  $(T - \Omega)$  is computed. Then this relationship is modeled by the following expression:

$$T = G + H\Omega^N \tag{16}$$

With T the torque value (Nm),  $\Omega$  the rotational speed (rad/s) and G (Nm), H (Nms), and N the constants of the model. After performing the series of simulations, G, H and N can be expressed in function of  $\tau_o$ , k, and n by mathematical regression. The regression method used for this step is

Figure 2: Variation of shear stress with shear rate according to the modified Herschel-Bulkley Model.

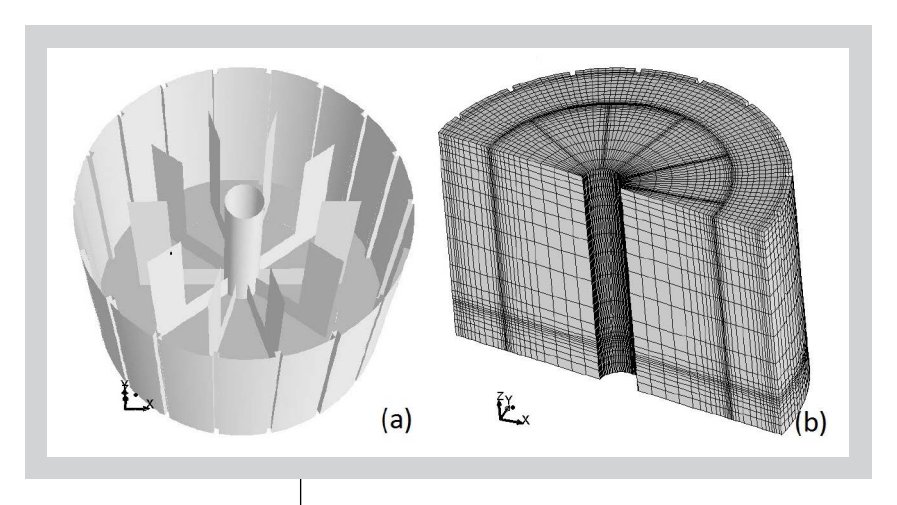


Figure 3 (left): (a) Geometry of the Contec viscometer and (b) meshing of the Contec viscometer.

Figure 4: Comparison of the numerical simulation (line - model equation on the left side) and experimentation (dot model equation on the right side) for mixture 3 and 5.

Table 1: Composition of mixture 3 and 5.

Table 2: Rheological properties of mixture 3 and 5.

Table 3: Error of the simulation value comparing to the experimentation value of G and H for the mixture 3 and 5.

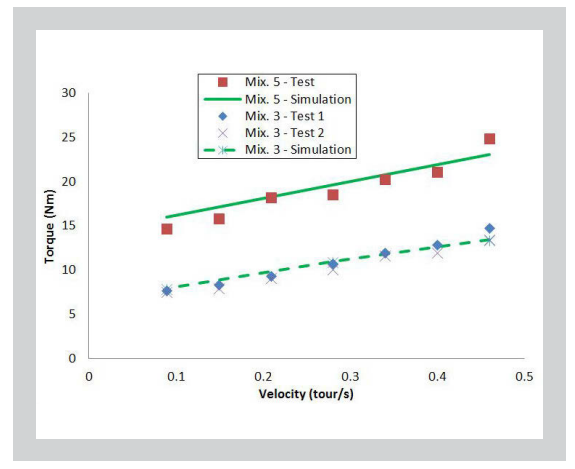
the so-called least square fitting [27]. Afterwards, by giving G, H and N their measured values, a system of three equations and three unknowns is obtained. Resolving the system allows to obtain the values of  $\tau_o$ ,  $\mu$ , and n.

For the simulation of the Tattersall MK-II, a wide variety of yield stress  $\tau_o$ , consistency k, and power index n was studied. The yield stress variation was 0, 20, 50, 75, 100, 125, 150, 200, 400 and 800 Pa (10 cases). The consistency variation was 5, 10, 20, 40, 60, 80, 100, 150 and 200 Pas (9 cases). The flow index n variation was 1, 1.1, 1.2, 1.3 and 1.4 (5 cases). The values of yield stress, consistency, and power index are proposed based on the experimental measurements for conventional concrete and self-compacting concrete realized in the earlier researches [28, 29]. The values of flow index are greater than or equal to 1 corresponding to Bingham or shear-thickening concretes. Since no shear thinning concrete has been reported in the literature, the flow index value

Composition (in kg/m³)	Mixture 3	Mixture 5
Ponteaux 10/16 Ponteaux 5/12.5 Estuaire 0/4 Cement Superplasticizer Water Target yield stress Target plastic viscosity	620 356 440 723 11.403 222 low high	1161 0 661 391 1.59 194 moderate moderate

	Mixture 3	Mixture 5
$ au_O$ (Pa)	408	911
K (Pas)	82.4	108.4
n	1	1
$\dot{\gamma}_C$ (1/s)	0.001	0.001

Test	Test 1	Test 2	Test 1
	Mixture 3	Mixture 3	Mixture 5
H simulated (Nms) H experimental (Nm) H error (%) G simulated (Nms) G experimental (Nm) G error (%)	14.975 18.954 20.1 6.5943 5.6083 17.6	14.975 16.329 8 6.5943 5.7608 14.5	19.004 24.659 22.9 14.296 12.224



less than 1 are not considered. For each single case of yield stress, consistency, and flow index, six simulations were performed at different rotational speeds which are 0.95, 2.54, 4.07, 5.61, 7.10, and 8.71 rad/s. These values are chosen based on the experimental rotational speed profile of the apparatus [10]. Thus, the total number of simulations is 10.9.5.6 = 2700. In order to do not manually repeat the simulations 2700 times, a workflow which is implemented into Fluent was made by editing the Fluent journal file.

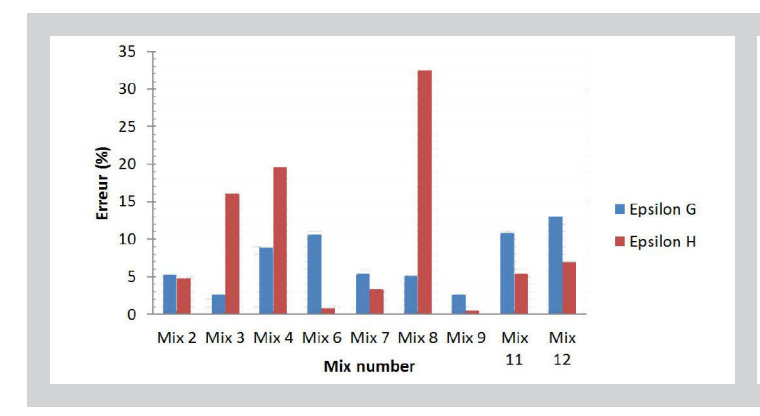
#### 4.4 CONTEC VISCOMETER 5 SIMULATION

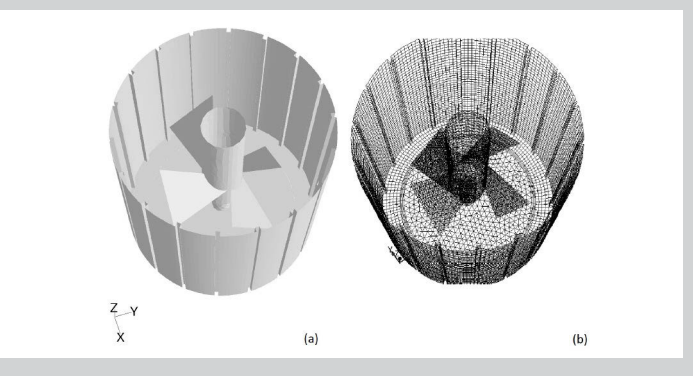
#### 4.4.1 Meshing

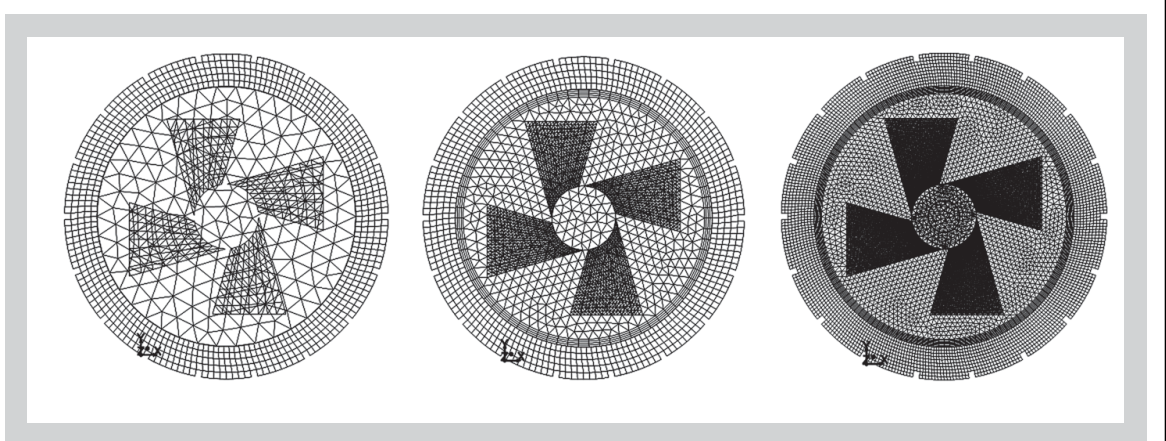
The inner cylinder of the Contec viscometer 5 has 10 rectangular blades positioned in parallel in the vertical direction, as shown in Figure 3a. The outer cylinder is equipped with 18 ribs in total. Because of the symmetrical geometry, it is possible to consider only one half of the whole domain containing 5 blades and 9 ribs. The computational domain is consequently only one half of the whole domain and is periodic in circumferential direction, meaning that all the flux going out of one cut plane is the flux going into its symmetry cut plane. The computational domain is filled with only hexahedral meshes rendering a highly structured mesh. All cells are high quality cells according to the Gambit mesh checking function. The sliding mesh is the cell zone limited by a cylindrical volume having the diameter and the height equal to these of the inner cylinder respectively. The cell size is refined gradually when getting closer to the interface between the moving mesh and the stationary mesh and to the free surface, as shown in Figure 3b.

#### 4.4.2 Simulation results

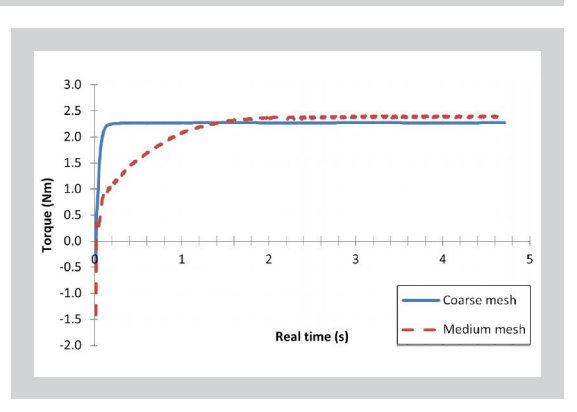
In order to test the accuracy of the Fluent solver and also to check for the use of the sliding mesh technique, we simulate two real tests which have been done for two concrete mixtures. The composition of these concrete is shown in the Table 1. Then we compare the computed torque-rota-







tional speed relationship to the measured one. The measured data were taken from the two tests performed with the Contec viscometer in a project of rheometers comparison which took place in Nantes, France [4]. The simulation takes into account the gravitational effect, the flow is set to laminar regime with no wall-slip condition, and the calculation runs in the transient (time dependent) mode. The two tests considered in the simulation are taken from the mixture number 3 and mixture number 5 which have the rheological properties described in the Table 2. For each mixture, seven simulations were performed at different rotational speed. For each rotational speed, a value of Torque (Nm) is registered. The comparison of the numerical Torque-rotational speed relationship to the measured one is presented in the Figure 4 for mixture 3 and mixture 5. The relative error of the simulated value comparing to the experimental value is calculated by the following expression: error  $\epsilon$  (%) =  $|v_{\text{sim}}|$   $v_{exp} / v_{exp} \cdot$  100 % and shown in Table 3. Where  $v_{sim}$ is the simulated value,  $v_{exp}$  is the experimental value. In these cases, the maximal error for H is 22.9 % and the maximal G error is 17.6 %. Of course the error in measuring G contributes to the error of H because of the linear regression. However, the deviation between the two real tests for the mixture 3 so called repetition error is already 13.8 % for the H value and 2 % for the G value. Moreover, the repetition error in a rheological test for concrete is quite high. Errors in the order from 10 to 20 % are common (see Figure 5,



data are collected from [4]). So generally, the simulation results agree quite well with the experimental measurements.

#### 4.5 TATTERSALL MK-II SIMULATION

#### 4.5.1 Meshing

Due to the complex positioning of the blades (Figure 6a), the complete domain must be meshed. The domain is divided into a sliding inner cylindrical domain and a stationary outer cylindrical domain. The sliding mesh is filled with tetrahedral cells and the outer domain is filled with hexahedral cells. To prevent low quality cells around the extreme angle of the blades, the diameter of the inner cylindrical domain is superior to the diameter of the vane. The cells are refined near the interface (Figure 6b). In order to study the influence of the cell size, three different meshes ranging from coarse, over medium to fine have

Figure 5 (left above): Repetition error of rheological tests for G and H with Contec viscometer 5.

Figure 6 (right above): (a) Geometry of the Tattersall MKII rheometer and (b) meshing of the Tattersall MKII rheometer.

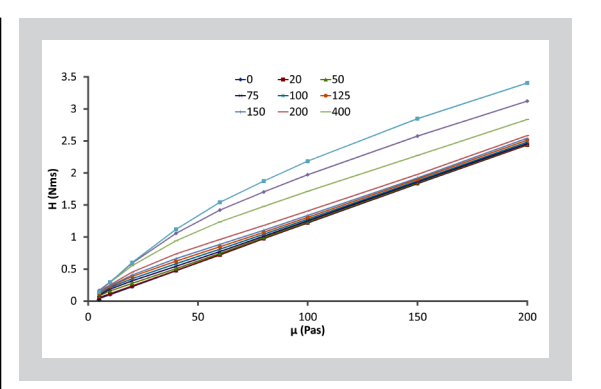
Figure 7 (middle): Meshing of the coarse mesh, medium mesh and fine mesh for the Tattersall MK-II rheometer.

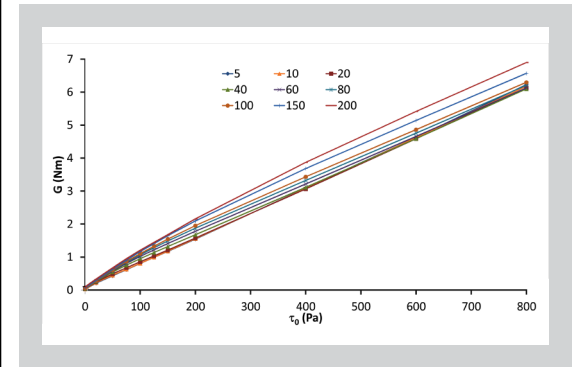
Figure 8 (right below):
Monitoring of computed
torque value during the calculation for the coarse mesh
and the medium mesh.

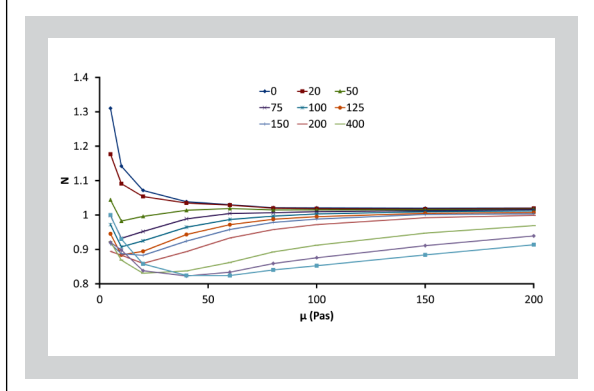
Figure 9 (above): Relationship between H,  $\tau_{\alpha}$ and  $\mu$  for the fluid going from o to 800 Pa in yield stress, o to 200 Pas in plastic viscosity and the power law index n = 1.

Figure 10 (middle): Relationship between  $G, \mu$ , and  $\tau_o$  for the fluid going from o to 800 Pa in yield stress, o to 200 Pas in plastic viscosity and the power law index n = 1.

Figure 11 (below): Relationship between N, o, and  $\mu$  for the fluid going from o to 800 Pa in yield stress, o to 200 Pas in plastic viscosity and the power law index n = 1.







been built with Gambit (Figure 7). The coarse mesh has 41612 cells, the medium mesh has 169428 cells, and the fine mesh has 1360620 cells. The objective of the mesh study is to choose the optimal mesh offering the best ratio between accuracy and computational time. The same simulation parameters have been set for the three meshes as follows: Material: Herschel-Bulkley material with  $\tau_0$  = 444 Pa, k =10.047, n = 1,  $\dot{\gamma}_c$  = 0.001, density = 2400 kg/m³, abd rotational speed = 0.96 rad/s. Transient flow and gravity effect have been taken into account. The value of the torque was monitored in function of the flow time. The fine mesh takes an extreme long time to converge and so was not studied anymore. Figure 8 shows the converged value of torque and the time long for the calculation to reach this value. The converged value of the torque is more accurate for the medium mesh than for the coarse mesh. The error is (2.41 - 2.28)/2.41 = 5%, however the computational time in case of the medium mesh is four to five times higher than for the coarse mesh. As the number of simulations to be done is very large (2700 simulations), the reduced

computational time of the coarse mesh is more important than the 5 % error which is certainly acceptable in this case. The final mesh taken into account is the coarse mesh.

#### Simulation results 4.5.2

For the simple geometry vane rheometers, it is typically sufficient to use the Reiner-Riwlin principle which provides two constants to be multiplied with G and H to obtain  $\tau_o$  and  $\mu$  respectively. This means that  $\tau_o$  and  $\mu$  both are a function of only one variable. After completing the 2700 simulations (corresponding to 450 materials), the simulation results of the Tattersall MK-II unfortunately show that one constant is not sufficient to describe  $\tau_o$  and  $\mu$ . In the appendix, the graphs resulting from the simulations show that G, H, and N are all depending on  $\tau_o$ ,  $\mu$ , and n. Hence,  $\tau_0$ ,  $\mu$ , or n all are a function of three variables G, H, and N. As a consequence, an analytical expression is required to describe such dependency. For this reason a regression plan is developed.

#### MODELING

#### 5.1 REGRESSION PLAN

The objective of the regression plan is to find out mathematical models allowing to express H, G, and N in function of  $\tau_o$ , k, and n. In order to express H in function of  $\tau_o$ , K, and n, we process in three phases. In the first phase, only the variation of  $\tau_o$  is considered in order to obtain a mathematical expression for H in function of  $\tau_o$ . This first expression includes some constants and  $\tau_o$ . In the second phase, the variation of *k* is included by expressing the constants in the first expression in function of k. At the end of this step, we obtain a second expression including constants,  $\tau_{o}$  and k. In the third phase we include the variation *n* into the second expression by extending its constants to become functions of n. At the end of this step, the final expression for H in function of  $\tau_o$ , k, and n is obtained. Following a similar way for G and N, we finally obtain three expressions that form a system as follows:

 $H = f_H(constants, \tau_o, k, n)$  $G = f_G(constants, \tau_o, k, n)$  $N = f_N(constants, \tau_o, k, n)$ 

By giving H, G, N a value, a system of three equations and three unknowns  $(\tau_{\alpha}, k, n)$  is obtained.

#### **5.2 MODELING RESULTS:**

For the case n=1 (Bingham fluid), the graphs showing the mathematical modeling and the raw data are given in Figures 14 to 16. For the others situation corresponding to n=1.1, n=1.2, n=1.3, n=1.4, similar figures have been obtained. The symbols show the raw data and the line curves are the mathematical modeling.

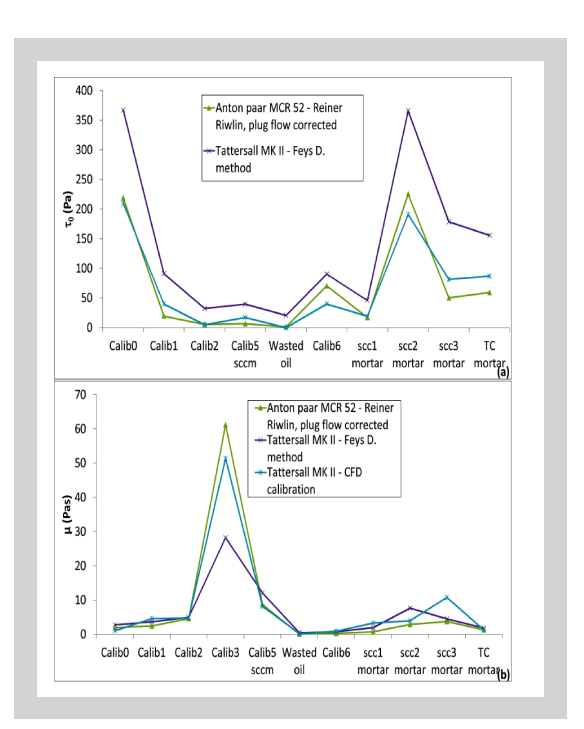
#### 5.3 EXPERIMENTAL MODELING VALIDATION

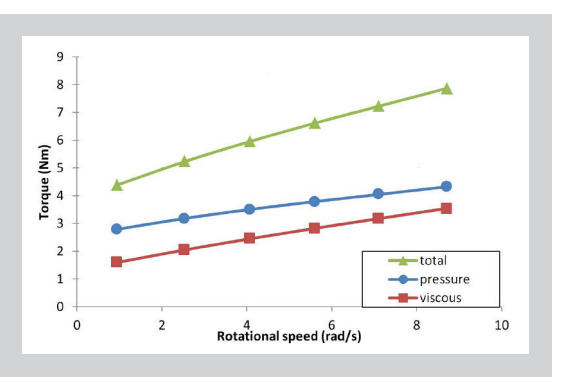
For the objective of validating the modeling results, an experimental test series has been defined. 10 fluids including 1 oil and 9 mortars have been prepared. The rheological measurement for each fluid was done by two rheometers: the Tattersall MK-II and the Anton Paar MCR-52. The comparison of the rheological parameters as obtained by the two rheometers is shown in Figure 12. For the Anton Paar MCR-52 rheometer, four methods have been used to obtain the flow curve from the T -  $\Omega$  curve (mentioned in the Section 3). However, only the Reiner-Riwlin with plug flow correction method is used in this comparison because it is considered to be the most accurate one. For the Tattersall MK-II, two methods have been used which are the "CFD-calibration" using the above modeling (Section 4.2) and the "Feys method" [10] mentioned in the Section 3. In general, the Tattersall MK II - CFD calibration method shows a good concordance with the other methods. Particularly it shows a very good agreement with the Anton Paar MCR 52 using the Reiner-Riwlin method including the plug flow correction, which is assumed to give the most accurate results.

#### 6 DISCUSSION

#### 6.1 CFD CALIBRATION METHOD

For measuring the rheology of mortar, the Anton Paar MCR 52 rheometer has an accurate measurement unit and simple geometry concentric cylinders that allow to apply the Reiner-Riwlin equation (Equations 7 and 8) without any problem. Moreover, a plug flow correction has been implemented into the calculation of shear stress and shear rate so the device definitely delivers





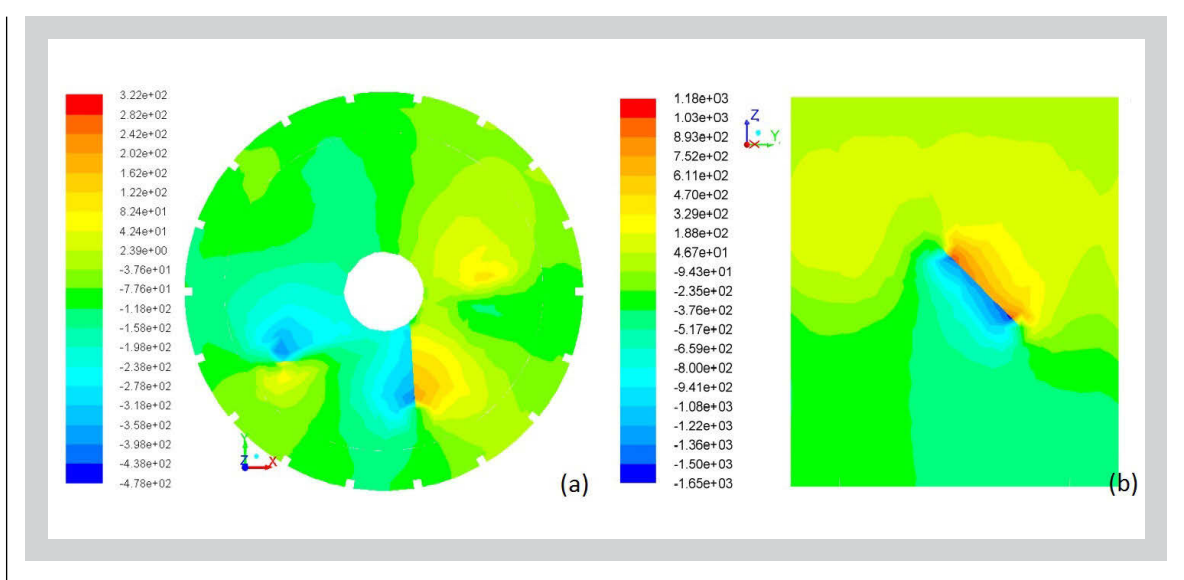
reliable results. Since we take those results as reference, in the Figure 12 we can observe that the results obtained with the CFD calibration method agreed with the results from the Anton Paar and therefore are more accurate than the other method. The old method of calibration of Feys et al. [10] consists of testing honey and oil (of which the rheological properties are known) and find out a multiplication factor to solve the inverse problem: "The torque (in Nm) must be multiplied with 124.37 in order to obtain the shear stress (Pa). The rotational velocity (in rot/min) is multiplied with 0.1931 in order to obtain the shear rate (1/s)". According to these results, shear strass and shear rate are given by  $\tau$  = 124.37 T and  $\dot{\gamma}$  =0.1931  $\Omega$ , repectively. That implies that  $k = dT/d\dot{\gamma} = d(124.37)$ T)/d(0.1931  $\Omega$ ) = 664.0704dT/ $d\Omega$  = 664.0704 Hand  $\tau_0$  = 124.37 G. This means that this method is based on the hypothesis that the consistency index k is a function of only one variable H and the yield stress is a function of only G. This is not correct (see Figures 9 to 11), the simulations show that both consistency index k, yield stress  $\tau_o$ , and flow index *n* are function of three variables: *H*, *G*, and N. That is the reason why there is a large discrepancies observed in the figures.

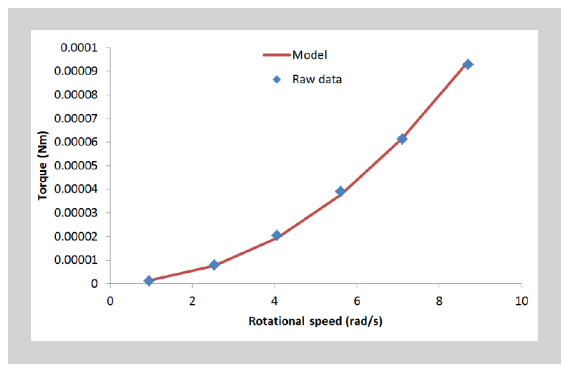
Figure 12 (above):
Comparison of experimental results of the (a) yield stress and (b) plastic viscosity obtained by different method on the Anton Paar MCR-52 rheometer and the Tattersall MK-II rheometer.

Figure 13:
The evolution of the total moment, the pressure moment and the viscous moment in function of the rotational speed for a false torque thinning case.

Figure 14 (above): The pressure distribution in the (a) horizontal cut plane and in the (b) vertical cut plane.

Fiaure 15: The variation of the torque in function of the rotational speed for the air in the FLUENT material library.





#### 6.2 FALSE SHEAR THICKENING AND SHEAR THINNING PHENOMENA

The results from the simulation show that for some materials, even if the material shows linear rheological behavior (n = 1) the T-N curve is not linear but shows torque thinning behavior. Also, an underestimated power index is observed for the shear thickening materials. The results from the simulation show that for some materials, even if the material shows linear rheological behavior (n = 1) the T-N curve is not linear but shows torque thinning behavior. Also, an underestimated power index is observed for the shear thickening materials. The computational torque value is computed from the summation of the moment resulting from the four blades around the rheometer axis. The total moment value is calculated by summing the product of the pressure force and the viscous force applied on the faces of the blades with the distances to the axis. Figure 13 shows an example for the evolution of the total moment, the pressure moment and the viscous moment in function of the rotational speed for a false torque thinning case. The material's rheological parameters are: yield stress = 800 Pa, consistence index = 40 Pas, power index = 1, and critical shear stress = 0.001. It is clearly observed that the nonlinear behavior of the total moment evolution is caused by both the viscous moment and the pressure moment.

Due to the form and the helical positioning of the blades, a vacuum zone is generated behind the blade (Figure 14) resulting in a negative pressure zone. The negative pressure zone will affect the moment magnitude and consequently induce an error on the torque. The magnitude of the error depends on the rotational speed and the fluid behavior. If the error increases nonlinearly with the rotational speed, then the moment (so the torque) increases nonlinearly with the rotational speed. On the other hand, the movement of the fluid through the blade is strongly affected by the rotational speed. Different trajectories of fluid particles are recorded while changing the rotational speed. This phenomenon can cause the variation of the force to become nonlinear. In consequence, false shear thinning and false shear thickening can be observed for a Bingham material or an underestimated power index is observed for a shear thickening material. The viscosity is the stickiness or the resistance of the flow. The lower the viscosity is, the easier the flow is. As a consequence, the phenomena in question are better pronounced in the zone of low viscosity than in the zone of high viscosity.

On the other hand, the particles have a tendency to move from the high pressure zone to the lower pressure zone. This flow causes a deviation of streamlines, resulting in a 3D flow. This indicates that the torque will be smaller than the expected value. This error also increases gradually while increasing the rotational speed. There may be a possibility that the error comes from the choice of the critical shear rate or the modified Herschel-Bulkley model (which is an approximation of the original Herschel-Bulkley model). In order to study this possibility, we simulate the flow of air in the rheometer. Air is a particular case of the Herschel-Bulkley fluid which does not require to specify the critical shear rate and has n = 1. Because the air is a Newtonian Fluid with very low viscosity and low yield stress so a clear

torque thickening is observed with n=2.1 (Figure 15). Of course, this phenomenon cannot be observed in the reality because the torque value is too small to be captured and is neglected regarding the internal friction of the rheometer. It confirms that the modified Herschel-Bulkley is not the cause of the false shear thickening, the false shear thinning and the underestimating n index phenomena. False shear thickening, false shear thinning and n index underestimation as mentioned above are taken into account when applying the mathematical regression modeling.

#### 7 CONCLUSION

In order to measure accurately the rheological properties of cement based materials with the Tattersall rheometer - a coaxial rheometer -, a numerical method has been developed. This method consists of simulating the operation of the rheometer with a wide range of known rheological fluid properties to obtain the relationship between the flow curve and the torquespeed curve. In order to use this relationship to accurately calculate the flow curve from the torque-speed curve of any unknown rheological properties fluid, this relationship has been modeled by doing mathematical fitting. The models obtained allow the employment of the method to be done quickly and accuracy. In order to investigate the accuracy of the method, an experimental comparison has been carried out between the Tattersall MK-II rheometer and the Anton Paar MCR52 rheometer which is a mortar rheometer having available formula to calculate the shear stress and shear rate. The comparison shows completely consistent results for the two rheometers. This method can be applied to other types of rheometer with complex geometry because it allows to take into account almost all of the potential errors including the end effect, the plug flow effect, the 3D flow of fluid through the blades and the vacuum zone behind the blades. Regarding its ability to get rid of the gravity-induced segregation, the Tattersall MK-II rheometer can be a quite polyvalent rheometer that can work for both concrete and mortar. However, the modeling does not perfectly fit for some cases of materials. As a consequence, an error is resulting. This error can be minimized by improving the mathematical fitting formula in future research.

#### **REFERENCES**

- [1] Wallevick OH, Gjorv OE: Development of a coaxial cylinder viscometer for fresh concrete, Proceeding of RILEM Colloquium, Properties of fresh concrete, Hannover (1990) 213 224.
- [2] Hu C, de Larrard F, Sedran T, Boulay C, Bosc F, Deflorenne F: Validation of BTRHEOM, the new rheometer for soft-to-fluid concrete. Materials and Structures 29 (1996) 620 631.
- [3] Jau WC, Yang CT: Development of a modified concrete rheometer to measure the rheological behavior of conventional and self-consolidating concretes. Cement & Concrete Composites 32 (2010) 450–460.
- [4] Ferraris CFB, Brower LE, Banfill P, Beaupre D, Chapdelaine F, de Larrard F. Domone P, Nachbaur L, Sedran T, Wallevik O, Wallevik JE: Comparison of Concrete Rheometers: International Tests at LCPC (Nantes, France), Nantes, France (2000).
- [5] Senff L, Hotza D, Labrincha JA: Effect of Lightweight Aggregates Addition on the Rheological Properties and the Hardened State of Mortars, Appl. Rheol. 21 (2011) 13668.
- [6] PereiradeOliveira LA, C.J., Nepomuceno M, The influence of wastes materials on the rheology of rendering mortars. Appl. Rheol. 23 (2013) 15505.
- [7] Yeow YL, Ko WC, Tang PPP: Solving the inverse problem of Couette viscometry by Tikhonov regularization, J. Rheol. 44 (2000) 1335–1351.
- [8] Ancey C: Solving the Couette inverse problem using a wavelet-vaguelette decomposition, J. Rheol. 49 (2005) 441–460.
- [9] Feys D, Wallevik JE, Yahia A., Khayat KH, Wallevik OH: Extension of the Reiner–Riwlin equation to determine modified Bingham parameters measured in coaxial cylinders rheometers. Materials and Structures 46 (2013) 289 – 311.
- [10] Feys D, Verhoeven R, De Schutter G: Evaluation of time independent rheological models applicable to fresh self-compacting concrete, Appl. Rheol. 17 (2007) 56244.
- [11] Estelle P, Lanos C: High Torque Vane Rheometer for Concrete: Principle and Validation from Rheological Measurements. Appl. Rheol. 22 (2012) 12881.
- [12] Tattersall GH, Banfill PJG: The rheology of fresh concrete, Pitman, Boston (1983).
- [13] Tattersall GH: The rationale of a two-point workability test. Magazine of Concrete Research 25 (1973) 169 172.
- [14] Tattersall GH, Banfill PJG: Further development of the two-point test for workability and extension of its range. Magazine of Concrete Research 31 (1979) 202–210.
- [15] Barnes HA: A handbook of elementary rheology, University of Wales, Institute of Non-Newtonian Fluid Mechanics, Aberystwyth: (2000).

- [16] Herschel WH, Bulkley R: Consistency measurements of rubber benzene solutions. Kolloid-Z. 39 (1926) 291-300.
- [17] Yahia A, Khayat KH: Analytical models for estimating yield stress of high-performance pseudoplastic grout. Cement and Concrete Research, 31 (2001) 731-738.
- [18] Banfill PFG: Rheology of Fresh cement and concrete. Rheology Reviews (2006).
- [19] Feys D, Verhoeven R, De Schutter G: Why is fresh self-compacting concrete shear thickening? Cement and Concrete Research 39 (2009) 510 - 523.
- [20] Nehdi M, Rahman MA: Effect of geometry and surface friction of test accessory on oscillatory rheological properties of cement pastes, ACI Materials Journal 101 (2004) 416 – 424.
- [21] Macosko CW: Rheology: principles, measurements, and applications, VCH, New York (1994).
- [22] Reiner M: Deformation and Flow: an elementary introduction to theoretical rheology, H. K. Lewis & Co., London (1949).

- [23] Barnes HA, Hutton JF, Walters K: An introduction to rheology, Elsevier, Amsterdam (1989).
- [24] Tanner RI, Walters K: Rheology: An historical perspective, Elsevier, Amsterdam (1998).
- [25] ANSYS FLUENT 12.0: User's guide, Section 8.4.5, 8-40.
- [26] Wallevik JE: Developement of parallel platebased measuring system for the contec viscometer, in RILEM international symposium on rheology of cement suspensions such as fresh concrete, Chicago (2009).
- [27] Trigeassou JC: Recherche de modèles expérimentaux assistée par ordinateur, Technique & Documentation Lavoisier (1988).
- [28] Kaplan D: Pompage des bétons, in Laboratoire Central des Ponts et Chaussées, Ecole Central des Ponts et Chaussées (2000).
- [29] Feys D: Interactions between Rheological Properties and Pumping of Self-Compacting Concrete, Ph.D. Thesis, Magnel Laboratory for Concrete Research, Ghent University, Ghent (2009).

